J Geophys (1987) 62:31–37

Journal of Geophysics

Seismic ground motion of sedimentary valleys – example La Molina, Lima, Peru

J. Zahradník [1] **and F. Hron** [2]

[1] Institute of Geophysics, Charles University, Ke Karlovu 3, 121 16 Praha 2, Czechoslovakia
[2] Institute of Earth and Planetary Physics, University of Alberta, Edmonton, Alberta T6G 2J1, Canada

Abstract. Strong motion accelerograms recorded at two sites in Lima, Peru, during the earthquake of November 9, 1974, exhibit serious dissimilarities although the sites have nearly the same epicentral distance. The two sites are the Instituto Geofísico del Perú in central Lima and the La Molina sediment-filled valley on the periphery of the city. The anomalously strong and prolonged ground motion at the La Molina site seems to be explained by a *combined* effect of the *complex topography of the bedrock* and the presence of *low-velocity subsurface sediments*. In contrast to an intuitive feeling, a strong velocity contrast along the whole sediment-bedrock interface is not necessary. Because severe earthquake effects in La Molina are of site origin, they should be expected to repeat in the future. As indicated by synthetic accelerograms, the anomaly refers to large areas of the La Molina valley and not only to the immediate vicinity of the recording point. For purposes of seismic microzoning and land-use planning, two microzones in the studied part of the valley will probably be appropriate.

Key words: Strong ground motion – Seismic microzoning – Local site effects – Sedimentary basins – Finite-difference method

Introduction

On November 9, 1974, at 12 h 59 m 49.8 s UT, an earthquake of magnitude $M_S = 7.2$ occurred in the Pacific, 12°30′ S, 77°47′ W (see Giesecke et al., 1980), at a distance of about 100 km from Lima. At two sites in the city (Fig. 1) the earthquake was recorded by standard strong motion accelerographs (Brady and Perez, 1977). While the first site, Instituto Geofísico del Perú (IGP) in central Lima, belongs to an area only weakly shaken by this earthquake as well as by previous earthquakes, the La Molina (MOL) site on the periphery is well known to be one of a few areas in Lima with extremely severe earthquake effects (Deza et al., 1976; Espinosa et al., 1977; J. Alva Hurtado, J. Kuroiwa, L. Ocola – personal communications). Correspondingly, the accelerograms from the IGP and MOL sites differ considerably.

In this paper we deal with low-passed (0–12.5 Hz) horizontal components (Fig. 2). The difference between the IGP and MOL components refers not only to peak acceleration values a_{max}, but to the whole wave pattern. The MOL record is of longer duration and exhibits sharp later onsets. In the next section, the explanation of these differences will be given in terms of local site conditions. For more details, see Zahradník and Hron (1986). Practical implications for earthquake engineering and land-use planning will then be given in the following section. The paper was stimulated by the fact that the campus of Universidad Nacional Agraria, located at the La Molina site, was much more heavily damaged than similar buildings in central Lima in 1970 and 1974. This fact calls for detailed investigations and decisive antiseismic measures.

Explaining the La Molina anomaly

In contrast to the weakly horizontally varying IGP subsurface structure, the MOL site is a complex (three-dimensional) sediment-filled valley. The bedrock is probably rep-

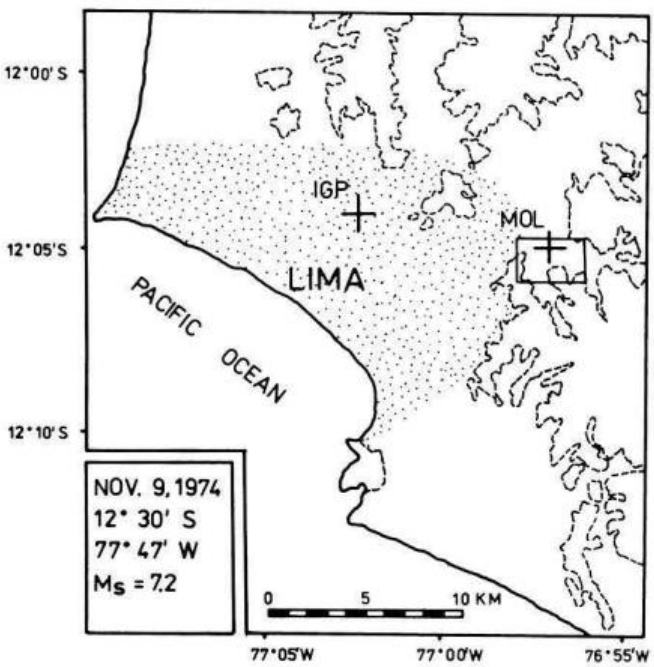

Fig. 1. Location of the IGP and MOL sites. The Lima territory is shown schematically as a *dotted area*. Surrounding hills are denoted by *dashed lines*. Parameters of the studied earthquake are given at *the left-hand corner*. A detailed map of the La Molina site (MOL) is given in Fig. 3

Offprint requests to: J. Zahradník

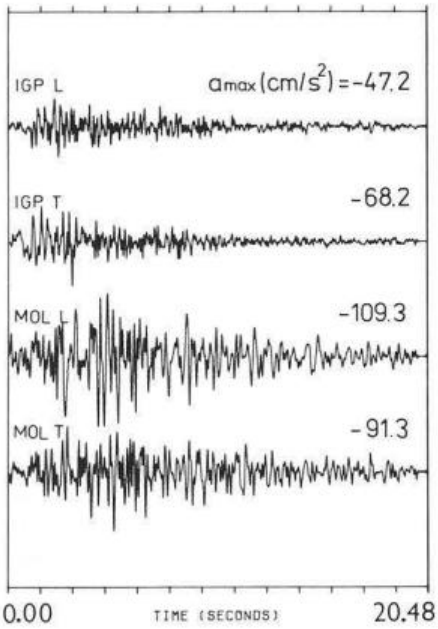

Fig. 2. Comparison of the low-pass filtered (0–12.5 Hz) accelerograms at the IGP and MOL sites of Lima, November 9, 1974; data from Brady and Perez (1977)

resented by hard crystalline rocks, as exposed on surrounding hills. Topography of the bedrock is approximately known from electrical resistivity measurements, as shown by the isolines in Fig. 3. Based on this map, we constructed eight cross-sections along linear profiles intersecting at the point where the La Molina strong motion accelerogram of November 9, 1974, was taken (Fig. 4). The intersection point is denoted by an arrow in each cross-section. Note that along some of the profiles the bedrock forms a local elevation, reaching the ground surface on profile 5 (see the small hill inside the valley in Fig. 3). This obstacle will be shown to play an important role in forming the seismic response of the whole site.

Sediments filling the La Molina valley are of Quaternary age. Their velocity-depth variation is not well known. We

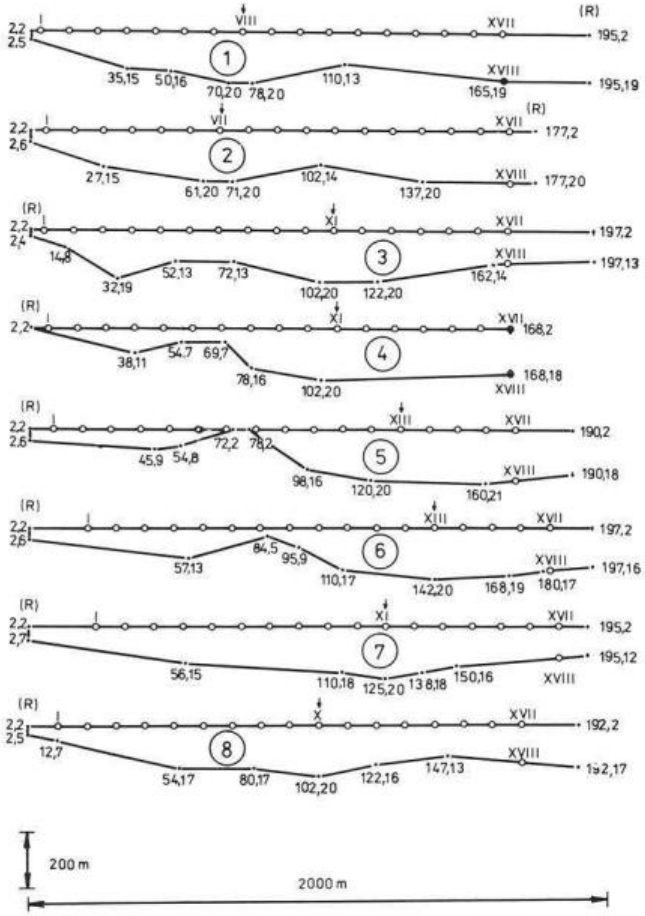

Fig. 4. Cross-sections of the La Molina basin along the individual profiles of Fig. 3 (their orientation shown by *R*). For the finite-difference method, the cross-sections are represented by polygons. Each corner is denoted by two integers, *NX* and *NZ*. The horizontal and vertical coordinates x and z of the corners (in metres) are given by $x=(NX-2)\cdot 10$ and $z=(NZ-2)\cdot 10$, respectively. *The bottom line* of each cross-section is the sediment-bedrock interface. *The open circles* indicate the locations ("receivers"), numbered I–XVIII, for which the synthetics were computed. *The arrow* on each profile marks the point of intersection of all eight profiles

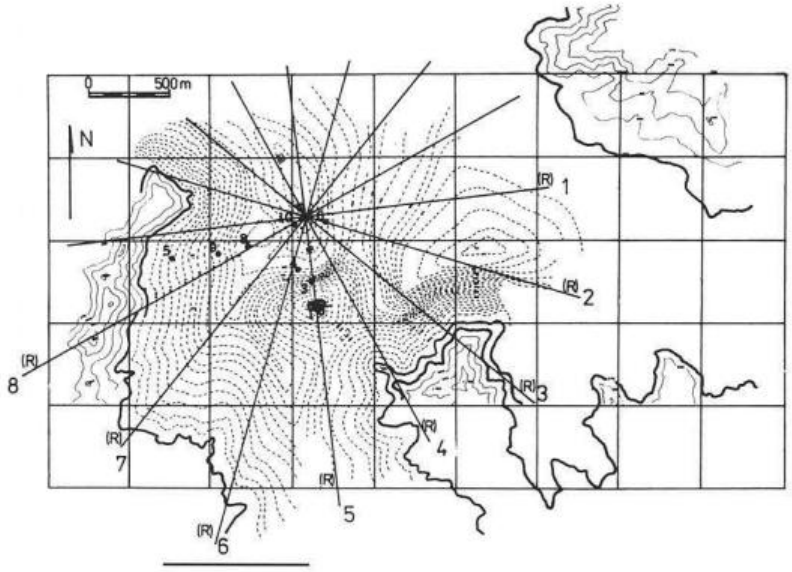

Fig. 3. The La Molina (MOL) site of Lima and eight radial profiles intersecting at the point of the strong motion recording station of November 9, 1974. The right-hand sides (*R*) of the profiles are shown, to which we refer in Fig. 4. The background map (after R. Benites, personal communication) illustrates the topography of the basin bottom by *dashed lines*; for a quantitative description see Fig. 4. The hills surrounding the sediment-filled basin are represented by *full lines*. *Numbered dots* denote the recording points of Tucker and Benites, mentioned in the text

only definitely know that the uppermost layer, about 10 m thick, is much less consolidated as compared to central Lima. It is likely that the same applies up to depths of about 50 m, as indicated by a few bore-hole data.

We attempt to explain the La Molina anomaly by computing synthetic accelerograms. The incompleteness of the subsurface data is believed to be at least partly compensated by extensive numerical experiments (more than 20 two-dimensional models and more than 500 synthetic accelerograms). Successful models, in which synthetics reasonably fit the specific features of the MOL record, serve for analysing physical factors influencing the ground motion. At the same time, they serve for extrapolating the ground motion from the recording point to the whole surface of the valley (points denoted by circles in Fig. 4).

The procedure is very simple. We start with the IGP record of November 9, 1974. Using a horizontally layered model of the IGP site and the simplest assumption of vertically propagating plane shear body waves, we deconvolve the surface record to obtain the acceleration time history of the *incident wave*. A possible IGP structure is shown by curve 3 of Fig. 5. This is a velocity-depth section for shear waves averaged from two extremes, labelled 1 and 2 in Fig. 5, proposed by P. Orihuela of IGP (personal communication). Figure 5 also displays the modulus of the IGP transfer function computed for model 3 by the matrix method. As the predominant frequencies of the November 9, 1974, accelerogram at IGP are 2.5–4.0 Hz (not shown here) and, since the transfer function varies slowly in that range, the incident waveform is very similar to that of the surface record. The whole difference can be well described by a factor 4 amplitude reduction. For this reason we do not present the incident wave graphically here.

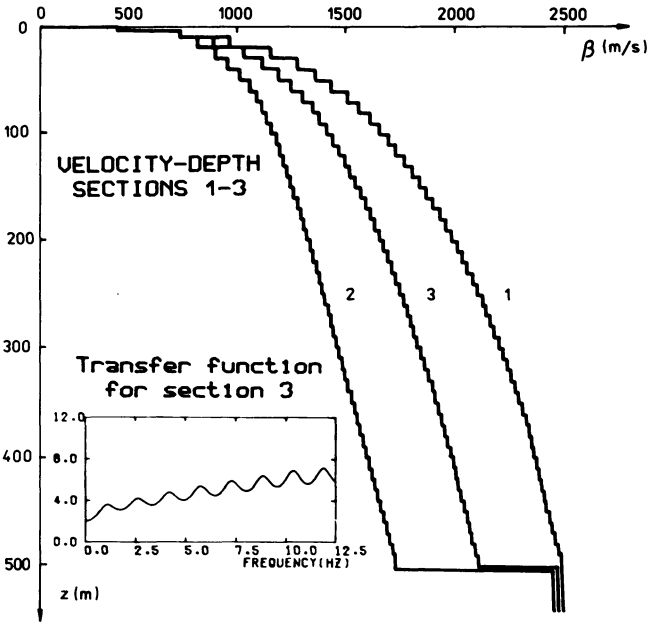

Fig. 5. Shear-wave velocity-depth sections. *Curves 1 and 2* represent two extremes (*curve 3* is their average) assumed for the IGP site. *The inset* shows the modulus of the transfer function corresponding to curve 3

Next, we assume the MOL site to be excited by the same incident wave, but now the wavefield is *numerically propagated upwards* and the individual two-dimensional La Molina cross-sections are analysed. The velocity-depth variation of the valley sediments is (optionally) taken into account. Only *SH* waves, vertical incidence, and non-absorbing media are considered for simplicity. The computational method based on finite differences is used (Zahradník, 1982, 1985; Zahradník and Urban, 1984). It consists of two steps. In the first one we compute an approximation to the impulse response of the basin using a simple delta-like impulse of short duration $T(=0.06$ or 0.08 s). In the second step we convolve this response with the incident wave. The space and time grid steps are $\Delta x=10$ m and $\Delta t=0.0027$ s, respectively. The method is of acceptable accuracy up to frequencies $f_{ac}=\beta_{min}/12\,\Delta x$, where β_{min} denotes the minimum shear velocity. With $\beta_{min}=500$ m/s in the models used, $f_{ac}\doteq 4$ Hz. Although relatively small, this value is sufficient for explaining the main features of the MOL record whose predominent frequencies are 1–4 Hz (MOL spectra are not shown here). This fact, together with the predominance of frequencies $f=2$–4 Hz in the incident wave mentioned above, makes it possible to retain formally in our synthetic accelerograms even frequencies $f>4$ Hz with low accuracy. In other words, the incident wave together with the structure act as a filter to suppress the numerical error connected with higher frequencies.

Obviously, this approach works well only when the numerical error has no character of spurious resonances (i.e. a strongly band-limited ringing). The resonance does occur in a vicinity of the highest frequency transmitted by the grid, $f_{cut\text{-}off}=\beta_{min}/2\,\Delta x=25$ Hz, if the impulse spectrum does not fall to zero for $f<f_{cut\text{-}off}$. Our impulse spectrum falls to zero at $f\doteq 3/T(=50$ or 37.5 Hz). To avoid the influence of the resonance close to 25 Hz we restrict ourselves to $f=0$–12.5 Hz only, i.e. frequencies beyond 12.5 Hz are filtered out from the impulse response, synthetic accelerograms, and also (for comparison) from the observed records.

As a consequence at $4<f<12.5$ Hz we have no accurate computations, but the error has no resonant character and, moreover, its influence is limited by the incident wave and the structure as explained above. Retaining $4<f<12.5$ Hz is advantageous because it makes a qualitative interpretation of the computed wavefield easier as compared to the case of filtering out all inaccurate frequencies; e.g., see, Figs. 9 and 10.

Three different classes of La Molina computational models were considered: (i) homogeneous basins with low-velocity sediments, (ii) two-layered basins with a relatively strong interface between the upper low-velocity and the lower high-velocity sediments and (iii) multilayered basins with a quasi-smooth velocity-depth increase (weak interfaces between the individual layers 10 m thick) and relatively high velocities in deep sediments. In *each class*, some successful models have been found, thus illustrating the non-uniqueness of the interpretation. However, *all together* they provide a strong indication of the primary role of the bedrock topography at the La Molina site. This will be shown here by three examples.

The first example, model 403, corresponds to a relatively low (500 m/s) *constant* shear-wave velocity in the sediments and cross-section 4; the bedrock velocity is supposed to be 2500 m/s. In Fig. 6 the synthetic accelerogram of this model is compared to the original IGP and MOL records. The synthetic is just for the point of intersection of the profiles (point XI of cross-section 4). We emphasize, of

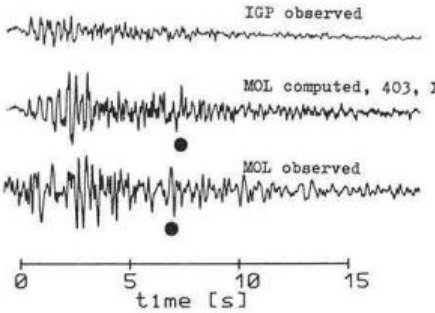

Fig. 6. Comparison of the observed IGP (*top*) and MOL (*bottom*) accelerograms with the synthetic MOL accelerogram computed for the receiver location XI of profile 4 (cf. Fig. 4) in model 403 (*middle*). Model 403 is the basin with *constant* sediment velocity. *The dots* indicate one of the later arrivals. We emphasize that *the middle trace* was obtained in the course of computation from the top one, without any knowledge of the bottom trace

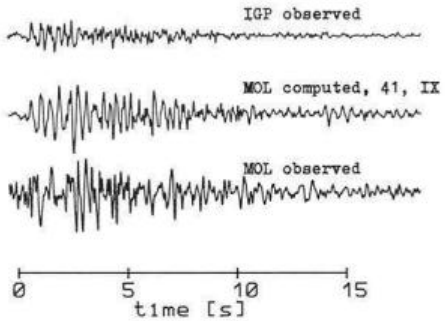

Fig. 8. The same as Fig. 6, but for receiver IX of profile 4 and model 41. Model 41 is the *two-layered* basin. Again, *the middle trace* was obtained from the top one, without any knowledge of the bottom "target" trace. For other examples with different models and profiles, see Zahradník and Hron (1986)

course, that what are plotted are the mutually shifted records (so as to give the best fit) because we do not know the actual time shift between the IGP and MOL original records. As seen from Fig. 6, the synthetic accelerogram fits not only peak acceleration well, but also the bell-shaped envelope and one of the sharp later onsets (see the dots). It can be shown, by a figure analogous to Fig. 9 presented below, that the success of model 403 is due to strong interference waves propagating horizontally from the valley edge, and also from the local bedrock elevation inside the valley. Such waves, interpreted as local surface waves by Bard and Bouchon (1980), result from overcritical reflections at the strongly inclined bottom. A necessary condition for a good fit with a homogeneous basin is the relatively low sediment velocity; otherwise the local surface waves are too weak.

To complete the presentation of model 403, synthetic accelerograms (left) and their normalized Fourier amplitude spectra (right) are given for the whole profile 4 in Fig. 7. The curves denoted 1, 2, 3, ... correspond to *odd* receivers I, III, V, ... of Fig. 4. Their discussion will be given in the next section.

The second example corresponds to the *two-layered* model 41, Fig. 8. It again refers to profile 4. The upper layer (50 m thick) now has a shear-wave velocity of 500 m/s and the velocity in the lower layer is 1500 m/s. The bedrock velocity is again 2500 m/s. Here a slightly better fit to the real MOL record was found with the synthetic accelerogram No. 5 (point IX) than with No. 6 (strictly equivalent to the recording point XI). In model 41 the local surface wave is even better developed than in model 403, and it dominates the wavefield. Because of the internal discontinuity in the sediments, this wave (L) is now *trapped* by the low-velocity subsurface layer acting as a *waveguide*. This can best be seen from the low-pass filtered impulse response (Fig. 9).

The response was computed with $T=0.06$ s. Although for further computation the response was filtered by means of a simple cosine taper between 10.7 and 12.5 Hz, for purposes of its qualitative interpretation we present another filtering in Fig. 9. In this case the filtering is realized through convolving the computed response with the impulse $g(t)=\sin(2\pi t/\tilde{T})-0.5\sin(4\pi t/\tilde{T})$, $\tilde{T}=0.24$ s. Such presentation is advantageous for two reasons: (i) $g(t)$ is not very long, thus the individual waves can be identified and (ii) using $g(t)$, the predominant frequency of which is near to 4 Hz, the frequencies $4<f<12.5$ Hz are sup-

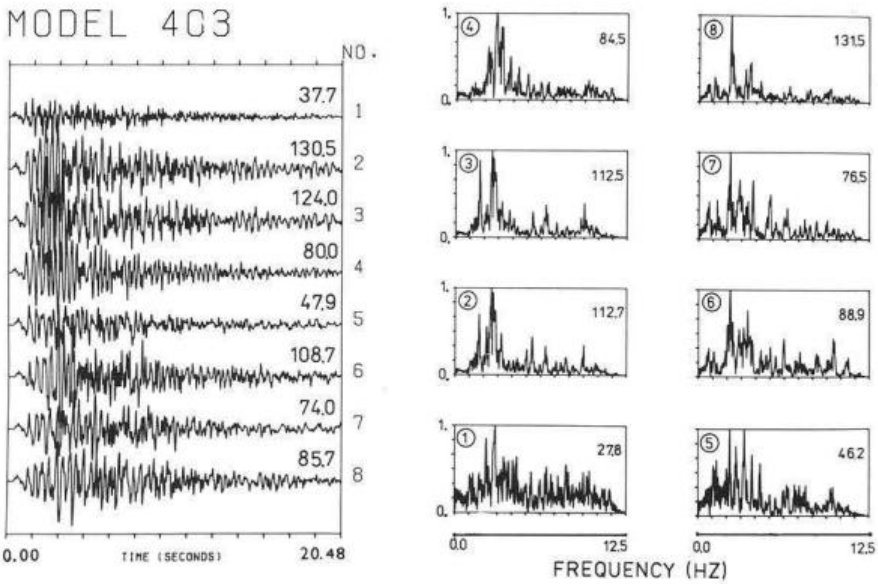

Fig. 7. Synthetic accelerograms (*left*) and their normalized Fourier amplitude spectra (*right*) of the La Molina basin model 403. The peak accelerations a_{max} in cm/s^2 and the actual maxima of the spectra, in cm/s, are given on the individual curves. *Curves 1, 2, ... 8* correspond to the *odd* receiver locations I, III, ... XV on cross-section 4 of Fig. 4

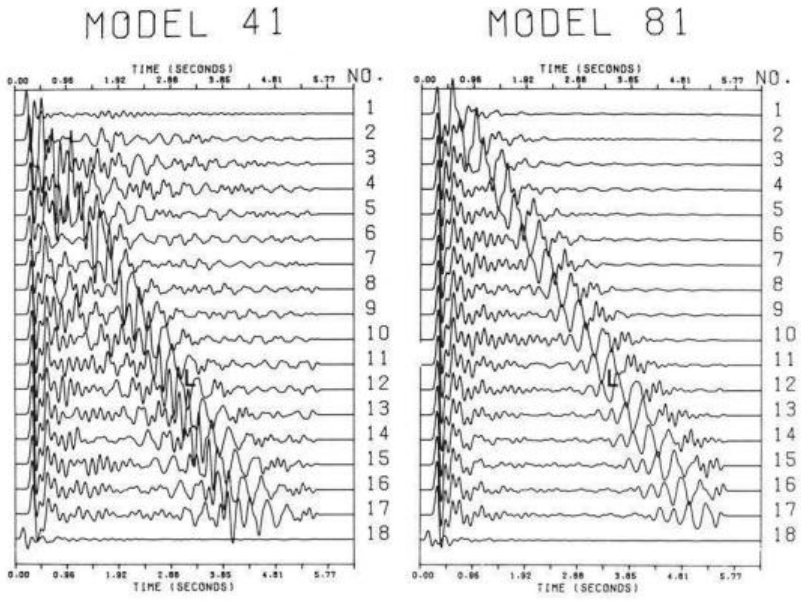

Fig. 9. The low-pass filtered (0–12.5 Hz) impulse responses computed for profiles 4 and 8 with *two-layered* models 41 and 81, respectively. For filter details see the text. *The curves labelled 1–18* correspond to locations I–XVIII of Fig. 4. *L* is the local surface wave generated at the edge of each cross-section (and, to a lesser degree, also at the local bedrock elevation of cross-section 4). The *L* wave dominates the wavefield because of the guiding effect of the upper low-velocity sedimentary layer of the models used. Note the long duration of the impulse response, caused by the *L* wave, explaining the observed long duration of the MOL accelerogram (cf. Fig. 8)

pressed in a similar way to the low-pass incident wave used for computing accelerograms. The fundamental, as well as the first higher waveguide mode, is evident from Fig. 9. Nevertheless, the sloping bedrock still represents the primary factor needed for developing the waveguide phenomenon. The same applies in general for all profiles, although each of them has its specific features corresponding to the bedrock geometry. See, for example, profile 8 (i.e. model 81, fully analogous to 41), included in Fig. 9 for comparison. The response of profile 4 is more complex due to its very shallow edge part and due to the local bedrock elevation.

The third example (Fig. 10) is to confirm the guided local surface waves even for *multilayered models* 432 and 832 with a *quasi-smooth* velocity-depth increase. Figure 10 refers again to profiles 4 and 8, but (in contrast to Fig. 9) the velocity-depth section of the valley sediments is now given by curve 2 of Fig. 5 and $T=0.08$ s is used. The cosine tapering between 10.7 and 12.5 Hz is used instead of convolving with $g(t)$ here. Thus the inaccurately computed frequencies $f>4$ Hz are less suppressed, but the individual waves are qualitatively better seen. The model also exhibits an interesting *focusing* of the reflected wave *R*, caused by the local bedrock depression below the points denoted by the arrow, e.g. at point *X* of profile 8, but *the role of this focusing is smaller than that of the wave L*. Note again the more complex response of profile 4 with respect to profile 8 (and also with respect to other profiles not presented here).

In other words, neither a very strong velocity contrast across the deep valley bottom nor a strong internal discontinuity inside the sediments is necessary for generating strong local surface waves. Instead, shallow low-velocity subsurface sediments overlying the steeply sloping bedrock at the edges of the valley (or in the vicinity of the local bedrock outcrop inside the valley) are sufficient. This is an important and generally valid finding of the present paper, a feature of sedimentary basins to which no sufficient attention has yet been paid by other investigators. Although the available geophysical data on the La Molina site are very sparse, it is quite definitely known that both conditions

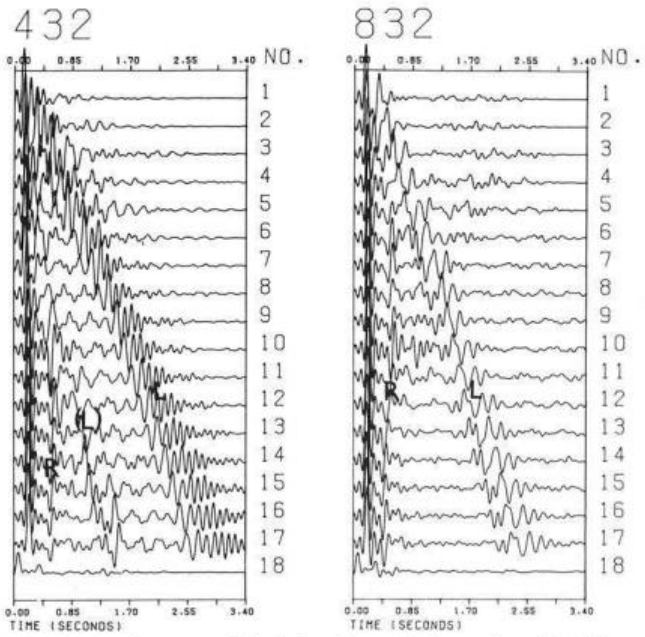

Fig. 10. Analogous to Fig. 9 but for *multilayered* models 432 and 832, respectively. For filter details, different from those of Fig. 9, see the text. *L* is the local surface wave, *R* is the wave reflected from the bedrock. Although the *R* wave exhibits a strong focusing effect, e.g. at point X of profile 8, the *L* wave still dominates the whole response. The *bracketed L*, (*L*), denotes the local surface wave generated on profile 4 at the local bedrock elevation

(i.e. very soft subsurface sediments and the steeply sloping bedrock beneath them) are fulfilled there. Consequently, it is very likely that strong local surface waves guided mainly in the uppermost sediments do play an important role at that site. It is just these waves of very small apparent velocities (like *L* in Fig. 9) that yield a significant *lenghtening* of the impulse response and, as a result, the prolongation of the accelerograms.

Another important fact is that the steeply sloping bedrock bounds the La Molina valley on several sides. Thus not only one, but several local surface waves originate

which (besides other effects) contribute to producing sharp late onsets. This applies probably to profiles 1 and 8 most strongly.

Before concluding this section, more attention should be devoted to the potential effect of *absorption*. Our computational method makes it possible to consider causal or non-causal absorption models, when neither β nor the phase velocity and the absorption coefficient depend on spatial coordinates. For basins with a spatially variable velocity, the non-causal (constant phase velocity) model with a spatially independent quality factor Q is easily applicable. The same approach as originally proposed for basins with absolutely rigid bottom may be used, as given by Eqs. (3)–(12) of Zahradník (1982). For more exact, but also more expensive, incorporation of absorption, see Emmerich and Korn (1987). We assumed that the effect of absorption is very large in the valley sediments, and thus we analysed several profiles taking absorption into account. However, in none of these models were we able to fit the observed MOL record; the synthetics were of smaller amplitudes and shorter durations than necessary, even though our Q was relatively large ($Q=40$). For this reason we do not present the synthetics with absorption here at all. Of course, this result is purely *formal* and by no means implies extremely high Q at the La Molina site. Rather, it means that the assumed velocities are wrong, or that neglecting the 3-D character of the valley in our 2-D computations makes the synthetics too weak. The latter explanation seems to be supported theoretically: the so-called transverse spreading of certain 3-D structures may have a strongly amplifying effect (Eq. 10.26, p. 102 of Červený, 1985), as lateral effects may lead to a contraction of ray tubes of the waves under consideration. We do not want to go into more detailed speculations here, but rather to analyse the effect of Q at another sedimentary basin where better data on shear velocities are available.

In summary, what probably makes the La Molina ground shaking so strong and long is the position of the site inside the valley of a complex bedrock topography (steeply sloping bedrock on several sides, and the inner bedrock elevation), together with the presence of surficial unconsolidated sedimentary layers. The layers themselves (i.e. without the sloping bedrock) would amplify the ground motion at selected frequencies, but they would probably never be able to prolong the ground motion as much as the La Molina site does.

Practical implications

Being of site origin, the severe earthquake effects should be expected to occur in La Molina repeatedly. Thus seismologists are forced to specify not only the expected differences of the La Molina ground motion with respect to central Lima, but to *microzone* the La Molina valley in detail. This is not the aim of this paper; thus we only intend to illustrate the efficiency of the computational approach to this problem. In fact, once we find a model for which the synthetics fit the La Molina record at most of the studied profiles, we can assume that the synthetics corresponding to other receiver positions in the same model also give a reasonable approximation to the actual La Molina ground motion. For example, in our case we have more than 100 synthetics (8 profiles) for the whole studied part of the valley, a number large enough to delineate areas of similar expected ground motions. Such an *extrapolation* seems to represent a very interesting feature of the computational approach to seismic microzoning problems, not widely used till now. Without going into details, we only emphasize that the microzoning map of the La Molina valley near the campus will probably be extremely *simple*, perhaps with *two microzones* only. We base this assumption on our present knowledge of several profiles, e.g. profile 4 in Fig. 7 where all synthetics (and their spectra) group into two classes only; type A – Nos. 2, 3, 4 and Nos. 6, 7, 8; and type B – No. 1, and No. 5. The synthetics of type A are strongly amplified and have a much narrower spectral band with respect to those of type B. Type A seems to be very common (on profile 4 as well as on the other profiles), thus indicating that the anomalous ground motion recorded on November 9, 1974, at one point in the valley was *not* a very local phenomenon of this point and its immediate vicinity, but rather that large areas of the valley behaved similarly. Of course, there is variability within type A too (see Fig. 7), but it is probably insignificant from the viewpoint of our knowledge of the subsurface geology and simplifying assumptions. Moreover, a more detailed microzoning would be impractical from the viewpoint of earthquake engineering. On the other hand, the difference between type A and type B is very large, and the transition between them quite abrupt (a factor 3 difference between accelerations No. 1 and No. 2 over a distance of only 200 m, as well as the broad-band and the narrow-band spectrum, respectively, Fig. 7), to justify their discrimination for practical purposes.

Our computational result of a very common occurrence of qualitatively the same (type A) seismic response in large areas of the La Molina site is consistent with the instrumental results of B. Tucker and R. Benites (personal communication). Based on simultaneous recordings of weak earthquakes at selected points of the La Molina valley (numbered points of Fig. 3), these authors derived ratios of spectra at the individual points with respect to point 1 at the rock outcrop on the small hill inside the valley. These ratios did not significantly differ from one point to another inside the valley.

In this respect the La Molina valley seems to behave similarly to the Chusal Valley, Garm (Tadjik SSR), but differently from the other valleys of the Garm region; see Tucker and King (1984).

We also mention that instrumentally determined spectral ratios were found to be practically independent of the earthquake azimuth (in Garm as well as in La Molina). Investigating azimuths different from those of the profiles, i.e. solving 3-D problems, represents serious difficulties for computational methods. In this respect, the instrumental methods are very useful. On the other hand, where applicable, the computational methods give better physical understanding of site anomalies.

Conclusion

The importance of local surface waves generated in sedimentary basins by earthquakes has been theoretically well established over the past years. This paper confirms their existence at a specific site, but also (and what is methodically more important) shows how relatively shallow low-velocity sediments strongly contribute to the generation and guiding of these waves. Our results also indicate that, in contrast to an intuitive feeling, a strong velocity contrast

along the *whole* sediment-bedrock interface is *not* necessary for making local surface waves intensive. Obviously, conditions for local surface waves being strong are probably fulfilled at many sites, including sediment-filled valleys with relatively high velocity gradients, since the presence of very soft surficial sediments above steeply sloping rocks at the edges of sedimentary basins is common enough.

A second point to emphasize is the efficiency of computational methods for extrapolating strong ground motions recorded at one or a few points of a sedimentary structure to the whole surface of the structure; a procedure valuable for seismic microzoning and land-use planning purposes.

Acknowledgements. The first-named author expresses his deepest gratitude to the Instituto Geofísico del Perú, Lima, and the Institute of Earth and Planetary Physics, Edmonton, for support and hospitality during his study visits to these institutions. The authors also thank two anonymous reviewers and G. Müller for their valuable comments which substantially helped them to improve the text.

References

Bard, P.Y., Bouchon, M.: The seismic response of sediment-filled valleys. Part 1. The case of incident SH waves. Bull. Seismol. Soc. Am. **70**, 1263–1286, 1980

Brady, A.G., Perez, V.: Strong-motion earthquake accelerograms, digitization and analysis; records from Lima, Peru: 1951 to 1974. Open-file report No. 77-587, U.S. Geological Survey, Menlo Park, 1977

Červený, V.: The application of ray tracing to the numerical modeling of seismic wavefields in complex structures. In: Seismic shear waves, G.P. Dohr, ed.: pp. 1–124, London: Geoph. Press 1985

Deza, E., Berrocal, J., Silgado, E., Rodriguez, A., Carbonel, C.: Intensidades observadas en Lima por el terremoto del 3 de Octubre de 1974 (informe). Instituto Geofísico del Perú, Lima, 1976

Emmerich, H., Korn, M.: Incorporation of attenuation into time-domain computations of seismic wavefields. Geophysics **52**, 1987 (in press)

Espinosa, A.F., Husid, R., Algermissen, S.T., De las Casas, J.: The Lima earthquake of October 3, 1974: intensity distribution. Bull. Seismol. Soc. Am. **67**, 1429–1439, 1977

Giesecke, A., Ocola, L., Silgado, E., Herrera, J., Giuliani, H.: El terremoto de Lima del 3 de Octubre de 1974 (informe). Lima: CERESIS/UNESCO 1980

Tucker, B.E., King, J.L.: Dependence of sediment-filled valley response on input amplitude and valley properties. Bull. Seismol. Soc. Am. **74**, 153–165, 1984

Zahradník, J.: Seismic response analysis of two-dimensional absorbing structures. Studia Geophys. at Geodaet. **26**, 24–41, 1982

Zahradník, J.: Programs for computing and analysing SH wavefields in two-dimensional absorbing block structures. In: Programs for interpreting seismic observations **3** (in Russian), N.N. Matveeva, ed.: pp. 124–186, Leningrad: Nauka 1985

Zahradník, J., Hron, F.: Earthquake ground motion at the La Molina sedimentary basin, Lima, Peru. Res. Report to CERESIS, Lima (60 pp., 18 figs., available on request) 1986

Zahradník, J., Urban, L.: Effect of a simple mountain range on underground seismic motion. Geophys. J.R. Astron. Soc. **79**, 167–183, 1984

Received December 1, 1986; revised version May 25, 1987
Accepted May 29, 1987